*Artificial Organs*
34(1):E1–E9, Wiley Periodicals, Inc.


# Analysis of Specific Absorption Rate and Current Density in Biological Tissues Surrounding Energy Transmission Transformer for an Artificial Heart: Using Magnetic Resonance Imaging-based Human Body Model

Naoya Higaki and Kenji Shiba

*Graduate School of Engineering, Hiroshima University, Higashi-Hiroshima-shi, Hiroshima, Japan*

**Abstract:** The transcutaneous energy transmission system used for artificial hearts is a transmission system that uses electromagnetic induction. Use of the TETS improves quality of life and reduces the risk of infection caused by percutaneous connections. This article reports the changes in the electromagnetic effects of TETS that influence a human body when the locations of the air-core coils of the transcutaneous transformer are changed. The specific absorption rate and current density in a model consisting of a human trunk that included 24 different organs are analyzed using an electromagnetic simulator. The air-core coils are located on the pectoralis major muscle near the collarbone in model 1, whereas they are located on the axillary region of the serratus anterior musle, which overlies the rib in model 2. The maximum current densities in models 1 and 2 are 5.2 A/m$^2$ and 6.1 A/m$^2$, respectively. The current density observed in model 2 slightly exceeds the limiting value prescribed by International Commission on Non-Ionizing Radiation Protection (ICNIRP). When the volumes of biological tissues whose current densities exceed the limiting value of current density for general public exposure are compared, the volume in model 2 (156.1 cm$^3$) is found to be larger than that in model 1 (93.7 cm$^3$). Hence, it is speculated that the presence of the ribs caused an increase in the current density. Therefore, it is concluded that model 1 satisfies the ICNIRP standards.
**Key Words:** Artificial heart—Transcutaneous energy transmission—International Commission on Non-Ionizing Radiation Protection—Specific absorption rate—Current density.

At present, the artificial heart is being further improved with respect to features such as durability and size (1,2). However, the energy is still supplied to the artificial hearts using cables (1–3). Hence, there is risk of infection in the region in the body where a wire passes through the skin and a consequent deterioration of quality of life (QOL) (3). Therefore, a transcutaneous energy transmission system (TETS) that transfers energy to the artificial heart by electromagnetic induction between the two air-core coils of a transcutaneous transformer has been developed; these air-core coils are placed facing each other on either side of the abdomen or chest (4–9). With the abovementioned TETS, QOL can be improved and the risk of infection due to percutaneous connections can be reduced. The first air-core transcutaneous transformers were developed in the early 1960s (4). Attempts have been made to design efficient air-core transcutaneous transformers that can operate under a wide range of conditions (6). However, in order to use this system for practical applications, it is necessary to investigate the electromagnetic influence of the TETS on biological tissue.

Shiba et al. in this article carried out electromagnetic analyses of the electric power absorbed by the body tissue and the current density in the body tissue to investigate the electromagnetic influence of the TETS on biological tissue (7). However, they considered the human body as a cylinder and considered only six biological tissues (skin, fat, muscles, small

doi:10.1111/j.1525-1594.2009.00916.x

Received May 2009.
Address correspondence and reprint requests to Dr. Kenji Shiba, Graduate School of Engineering, Hiroshima University, 4-1 Kagamiyama 1-chome, Higashi-Hiroshima-shi, Hiroshima 739-8527, Japan. E-mail: shiba@bsys.hiroshima-u.ac.jp

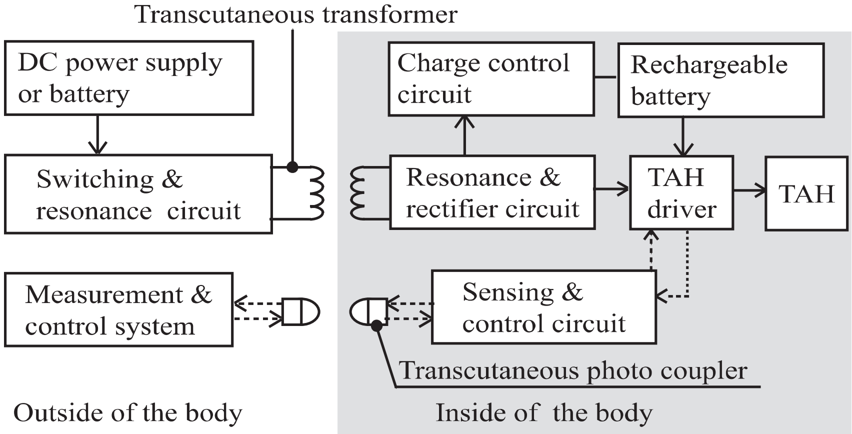


**FIG. 1.** Block diagram of the TETS for total artificial heart (TAH).

intestine, bone, and blood), and did not conduct sufficient analyses.

In this study, we performed an electromagnetic simulation using a model of the human trunk in order to investigate the influence of energy transmission on biological tissues; the abovementioned human trunk model contained 24 types of biological tissues. This model—a realistic high-resolution whole-body voxel model of a Japanese adult male with average height and weight—was developed by the National Institute of Information and Communications Technology in Japan (NICT) (10). Then, we considered the electromagnetic influence of TETS with an air-core coil arrangement on biological tissue.

## ENERGY TRANSMISSION SYSTEM

A block diagram of the TETS is shown in Fig. 1. Direct current supplied by a DC power source or a secondary battery placed outside the body is converted to alternating current of 100–1000 kHz using a switching circuit. The AC power is then transmitted inside the body by electromagnetic induction between the two air-core coils of the transcutaneous transformer. The AC power transmitted inside the body is reconverted to DC power using a rectifier circuit implanted in the body. Then, the DC power is supplied to the actuator of the artificial heart and the backup secondary battery.

The air-core transcutaneous transformer examined in this study is shown in Fig. 2. It consists of an external air-core coil that is set outside the body and an internal air-core coil implanted under the skin. The outer diameter, inner diameter, and thickness of the external air-core coil (35 turns) are 90, 20, and 1 mm, respectively. The outer diameter, inner diameter, and thickness of the internal air-core coil (20 turns) are 60, 20, and 1 mm, respectively (7).

## INFLUENCE OF ELECTROMAGNETISM

Electromagnetic influences of the TETS on biological tissue include thermal effects and stimulant action. The former is a result of Joule heating, whereas the latter caused excitation of the neurons and muscles by the induced current. The thermal effect is measured in terms of specific absorption rate (SAR; W/kg), whereas the stimulant action is indexed by current density $J$ (A/m$^2$). SAR is expressed as

$$SAR = \frac{\sigma E^2}{\rho} \tag{1}$$

where $E$ is the root mean square (RMS) electric field (V/m); σ, the electrical conductivity of the biological tissue (S/m); and ρ, the density of the biological tissue (kg/m$^3$). SAR is represented as an average value for 10 g of the tissue in each organ.

$J$ is expressed as

$$J = \sigma E \tag{2}$$

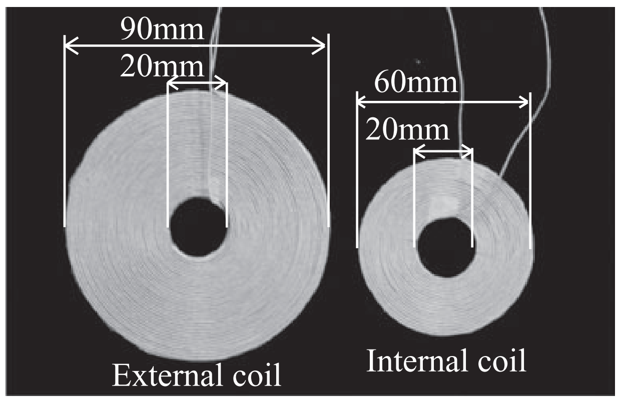


**FIG. 2.** Air-core transcutaneous transformer used in this study.

**TABLE 1.** *Limits for time-varying electric and magnetic fields of 100 kHz to 10 MHz (ICNIRP, 1998)*

| | Frequency range | Localized SAR (head and trunk) (W/kg) | Current density for head and trunk ($mA/m^2$) |
|---|---|---|---|
| Occupational exposure | 100 kHz–10 MHz | 10 | $f/100$ |
| General public | 100 kHz–10 MHz | 2 | $f/500$ |

$f$, frequency (Hz); SAR, specific adsorption rate.

$J$ is represented as an average value for 1 g of the tissue in each organ. Table 1 lists the basic requirements for the values of SAR and current density as prescribed by the International Commission on Non-Ionizing Radiation Protection (ICNIRP). The SAR averaging mass is defined as any 10 g of biological tissue. The $J$ values are averaged over a cross-section (1 $cm^2$) of the tissue perpendicular to current direction (11). The average $J$ value thus obtained corresponds to the mean value obtained for 1 g of biological tissue. We determine the electromagnetic influences of the TETS on a human body by comparing the values of SAR and $J$ obtained herein with their values specified by the ICNIRP.

## METHODS

### Transmission-line modeling method (TLM method)

Micro-Stripes (AET, Inc., CST AG, Darmstadt, Germany), an electromagnetic simulator whose operation is based on the TLM method (12), is used to estimate the SAR and $J$ values. The TLM method is a very powerful tool for field computations. The TLM method is based on an analogy between the electromagnetic field and a grid of transmission lines. A mathematical derivation of the TLM method can be directly obtained from a full wave time-domain solution of Maxwell's equations.

The analytical procedure using Micro-Stripes is as follows. First, we create a model of the human body with corresponding electrical characteristics. Next, we divide this model into small cells to form a mesh and calculate the electric field $E$, magnetic field $H$, and SAR. $J$ is then estimated using Eq. 2 by the analysis mentioned previously.

### Human body model based on magnetic resonance imaging (MRI) data

The human body model used for the analysis is shown in Fig. 3. We used the human body model developed by NICT; the size of this model is that of an average Japanese adult male (10). However, the numerical human body model developed by NICT cannot be imported directly into our simulator because the memory size, analysis time, and file format of the model developed by NICT were incompatible with those required by the simulator. Therefore, the basic model developed by NICT is first converted to a general three-dimensional CAD file format. Then, only the trunk of the model is extracted and used for our analysis.

The biological tissues of a human body model could be 24: cerebrospinal fluid, gall bladder, blood, small intestine, prostate-seminal vesicle, testis, pancreas, thyroid, stomach-duodenum, esophagus, muscle, trachea, heart, large intestine, kidney, bladder, skin, lung, spleen, fat, bone, and air in a trachea. This study uses $\sigma$ and relative permittivity $\varepsilon_r$ values defined by *Istituto di Fisica Applicata "Nello Carrara"* (IFAC) (13). The density of the organs is set to an average value of 1000 $kg/m^3$ for living body tissues, except for bones; the bone density is set to 2000 $kg/m^3$. The relative magnetic permeability is set to 1 for all the organs (14). The maximum mesh interval is $2 \times 2 \times 2$ mm, and the human body model is divided into $7.6 \times 10^5$ cells.

### Model for numerical analysis

The shapes of the air-core coils are shown in Fig. 4a. The separation between the air-core coils is 5 mm. The silicone layer is 3 mm thick. The internal air-core coil is attached to the fat tissue. An equivalent circuit for the analysis model is shown in Fig. 4b. In the equivalent circuit, the current $I_1$ in the external air-core coil, terminal voltage $V_{L1}$ of the external air-core coil, current $I_2$ in the internal air-core coil,

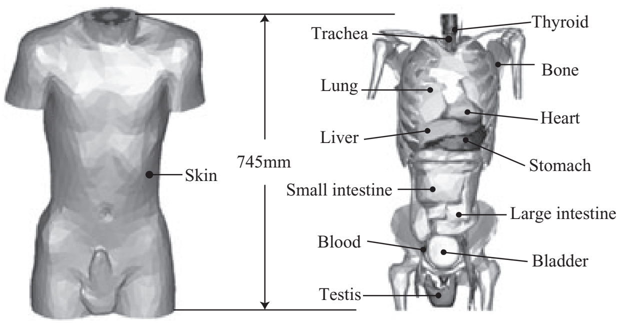


**FIG. 3.** Human body model for numerical analysis.

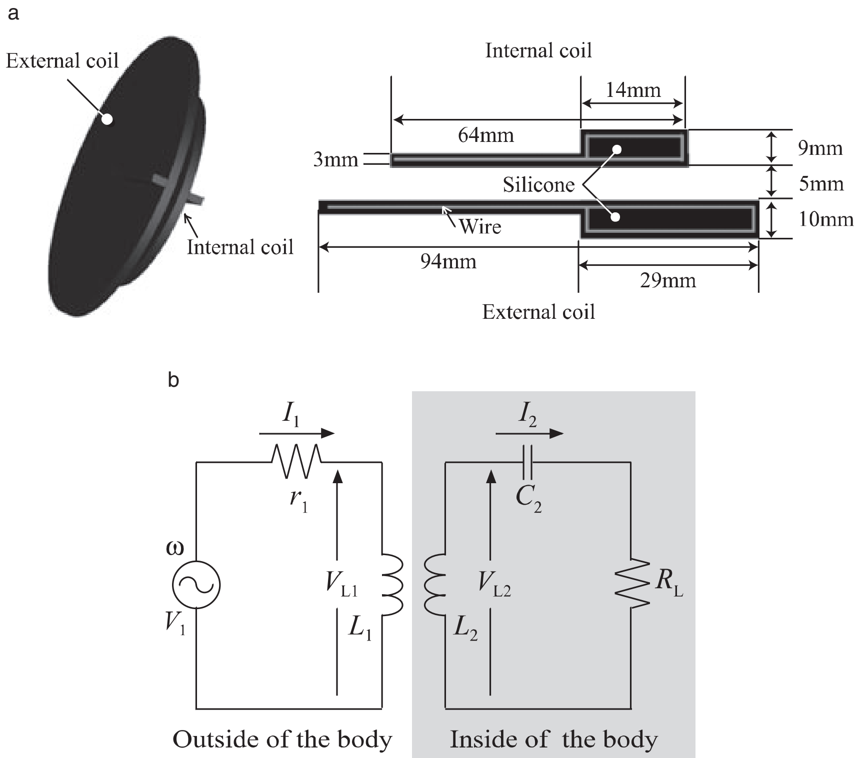


**FIG. 4.** Air-core coils for numerical analysis. (a) Shapes of air-core coils. (b) Equivalent circuit.

terminal voltage $V_{L2}$ of the external air-core coil, load resistance adjusted power supply voltage $V_1$, resistance $r_1$, and resonant capacitor $C_2$ are so adjusted that the results obtained are consistent with those obtained using the coil. The transmission conditions are adjusted so as to obtain an output electric power of 20 W and a transmission frequency of 600 kHz, which are conventionally considered to be safe for use in research (7).

In this study, we considered the changes in the electromagnetic influence of the TETS on biological tissues by changing the positions of the air-core coil. Figure 5a shows the analysis model (model 1) in which the air-core coils are set on the pectoralis major muscle near the collarbone. Figure 5b shows the analysis model (model 2) in which the air-core coils are located on the serratus anterior muscle of axilla on the rib. The arrangements of the coils in models 1 and 2 correspond to the setup of the TETS that is used for the artificial heart (15,16).

## ANALYSIS RESULTS

### SAR

The maximum values of SAR for each organ are shown in Fig. 6. The organs are listed in the descending order of their SAR values. Here, the dotted lines indicate the limit prescribed by ICNIRP for general public exposure. The three highest values of SAR in model 1 are obtained for the muscle, fat, and bone tissues (Fig. 6a). The three highest values of SAR in model 2 also correspond to those of the fat, muscle, and bone tissues (Fig. 6b). Thus, it is observed that SAR of the internal organs that are close to the body surface is higher than that of the organs away from the surface. The SAR values obtained in this study are well below the limit prescribed by the ICNIRP for general public exposure.

### *J* (Current density)

The maximum *J* values observed for each organ are shown in Fig. 7. The organs are listed in the descending order of their *J* values. Here, the upper and lower broken line indicate the basic restrictions imposed by the ICNIRP for occupational exposure and general public exposure, respectively. The five highest values of SAR in model 1 correspond to those of the skin, muscle, fat, lung, and blood tissues (Fig. 7a), whereas the five highest values of SAR in model 2 correspond to those of skin, muscle, lung, fat, and liver tissues (Fig. 7b). *J* values of the skin, muscle, and fat tissues in model 1, and those of the skin, muscle, fat, lung, and blood tissues in model 2 exceed the limit for general public exposure prescribed by the ICNIRP.

Figure 8 shows the biological tissues whose *J* values exceed the limits for general public exposure.

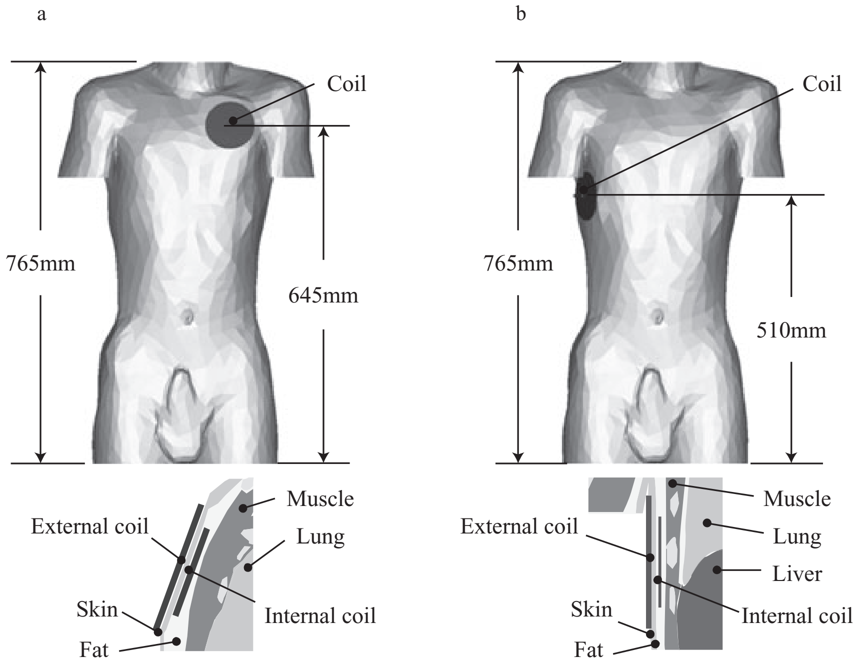


**FIG. 5.** Analyzed models. (a) Model 1 and (b) Model 2.

The volume of these tissues is 93.7 $cm^3$ in model 1 (Fig. 8a) and 156.1 $cm^3$ in model 2 (Fig. 8b). Thus, it can be said that the electromagnetic influence of the TETS on biological tissue is more pronounced in model 2 than in model 1.

## DISCUSSION

The three highest values of SAR in Fig. 6 correspond to those of the muscle, fat, and bone tissues. The three highest *J* values correspond to those of the

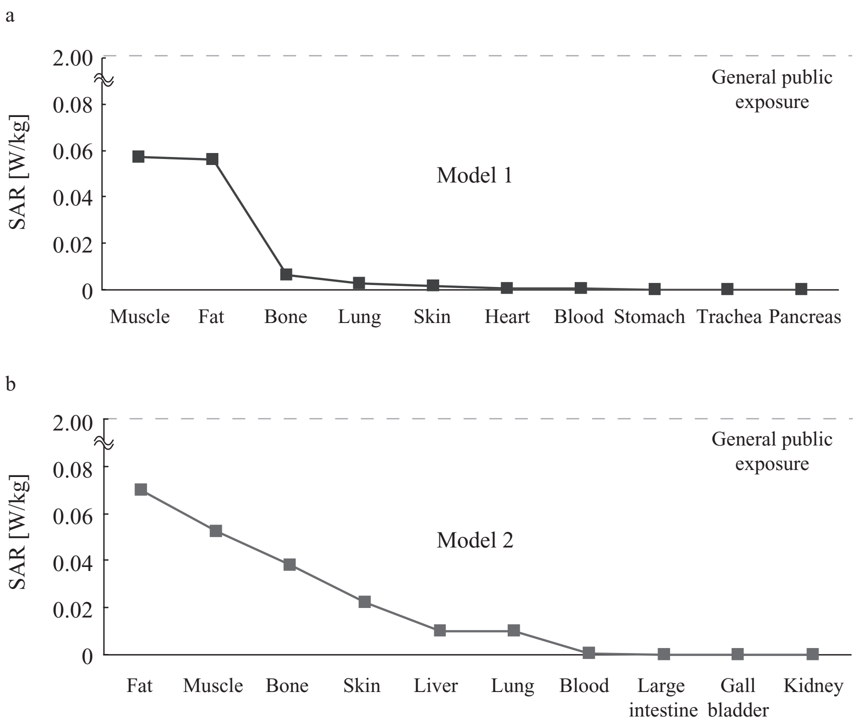


**FIG. 6.** SAR obtained for (a) Model 1 and (b) Model 2.

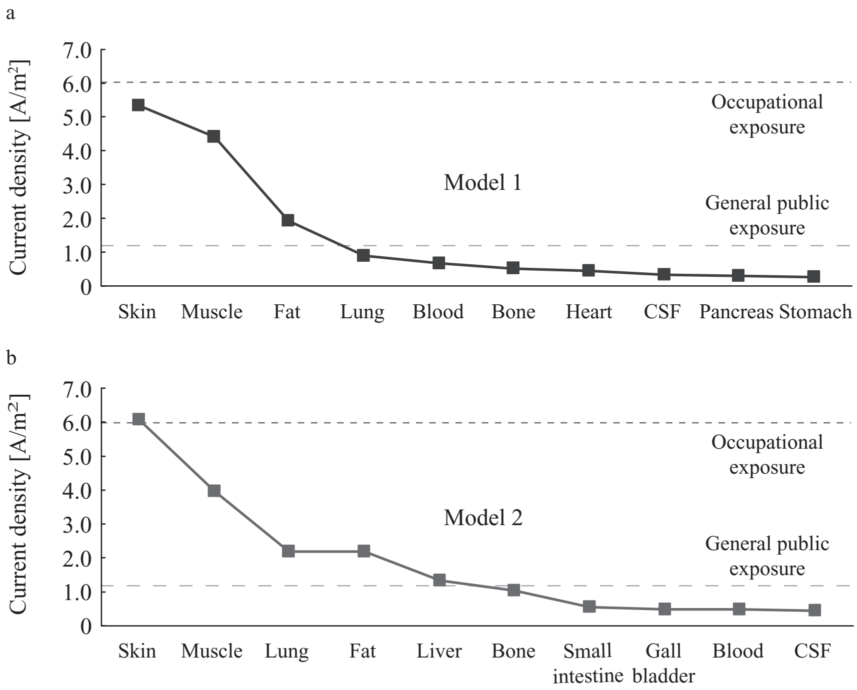


**FIG. 7.** Result of analysis of *J*. (a) Model 1 and (b) Model 2. CSF, cerebrospinal fluid.

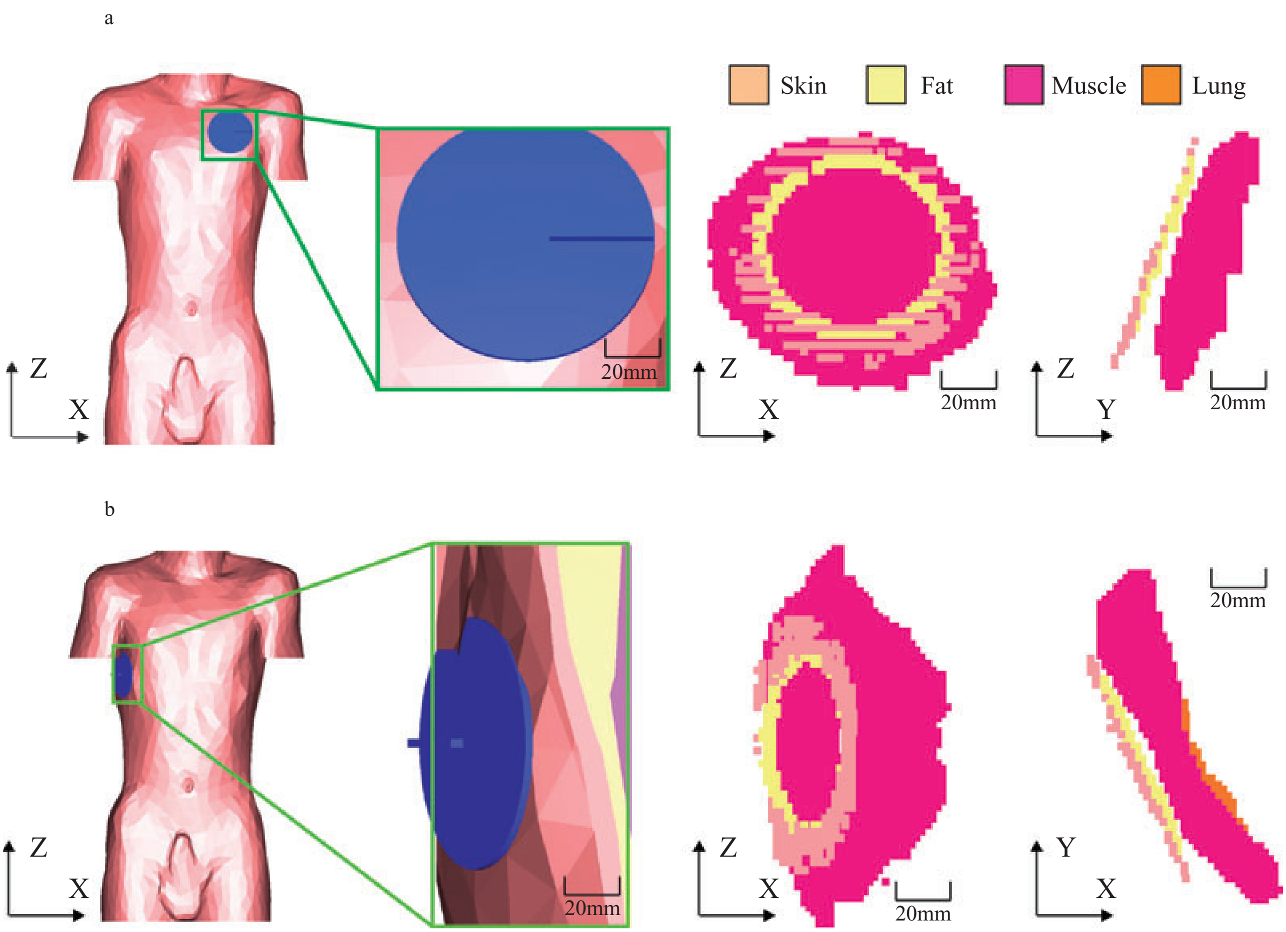


**FIG. 8.** *J* values obtained for (a) Model 1 and (b) Model 2.

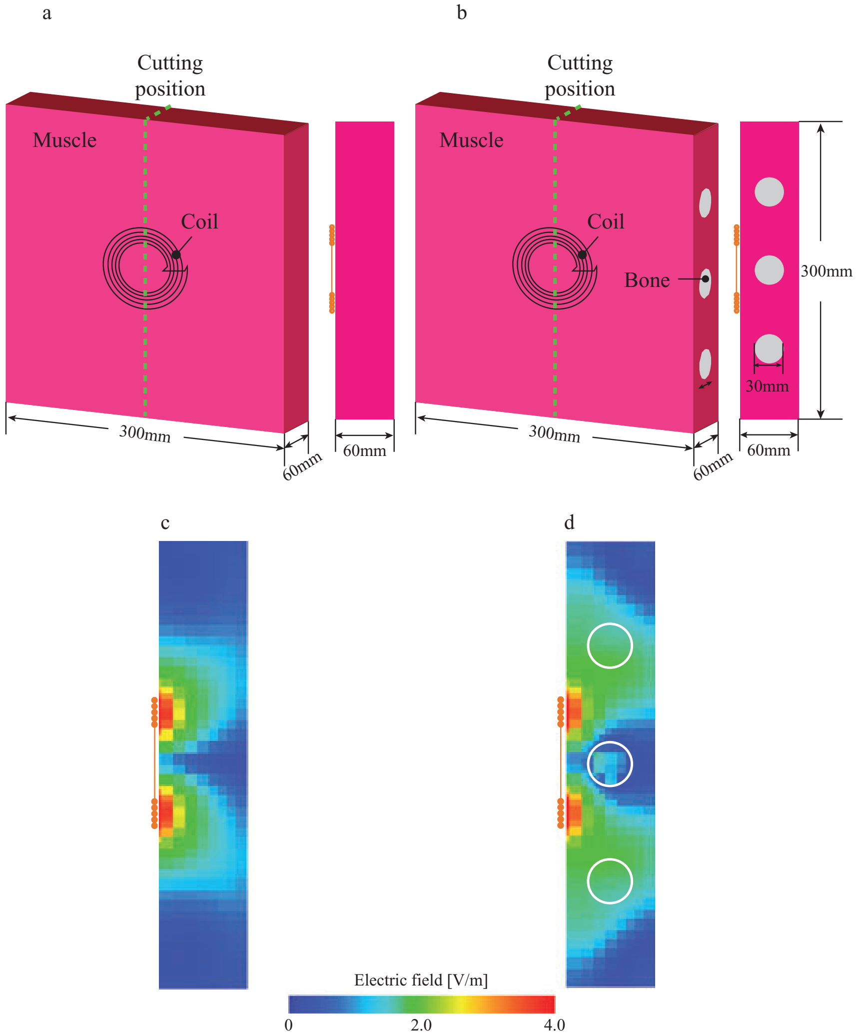


**FIG. 9.** (a) Simple model 1. (b) Simple model 2. (c) Simulation results for electric field distribution of simple model 1. (d) Simulation result for electric field distribution of simple model 2.

muscle, skin, and fat or lung tissues. The main reason for this difference between SAR and $J$ values is that SAR is averaged for every 10 g of tissues, whereas $J$ is averaged for every 1 g of tissues. According to the ICNIRP guidelines, if thermal diffusivity is considered when calculating SAR, then it is preferable, from a physiological point of view, to use an average value for 10 g of tissues (17).

From Fig. 6, it can be seen that the values of SAR are well below the ICNIRP limit for general public exposure. However, the $J$ values exceed the ICNIRP limit for general public exposure. The corresponding biological tissue's volume in model 1 and model 2 whose current density values exceed the restrictions for general public exposure are compared. It is seen that the volume of these tissues is greater in model 2 than in model 1. The major reason for this seems to be the location of the air-core coils. In model 1, the air-core coils are located on the pectoralis major muscle, whereas they are located on the serratus anterior muscle in model 2. Pectoralis major is a thick muscle, whereas serratus anterior is a complex muscle attached to the ribs. The serratus anterior muscle overlies the ribs. $E$ increases around a tissue with low conductivity or relative permittivity, such as fat tissues or bones, because reflection is repeated on those tissues from which conductivity or relative permittivity are greatly different, such as a bone and muscle or fat or muscle. We assume that the high electric field around an organ with low conductivity or relative permittivity, such as fat or a bone, results in an increase in $J$.

In order to confirm this phenomenon, we constructed some simple models, as shown in Fig. 9, and analyzed them. Simple model 1 consists of only muscle and the air-core coil (Fig. 9a). Simple model 2 is obtained by adding three bones to the simple model 1 (Fig. 9b). The muscle whose conductivity or

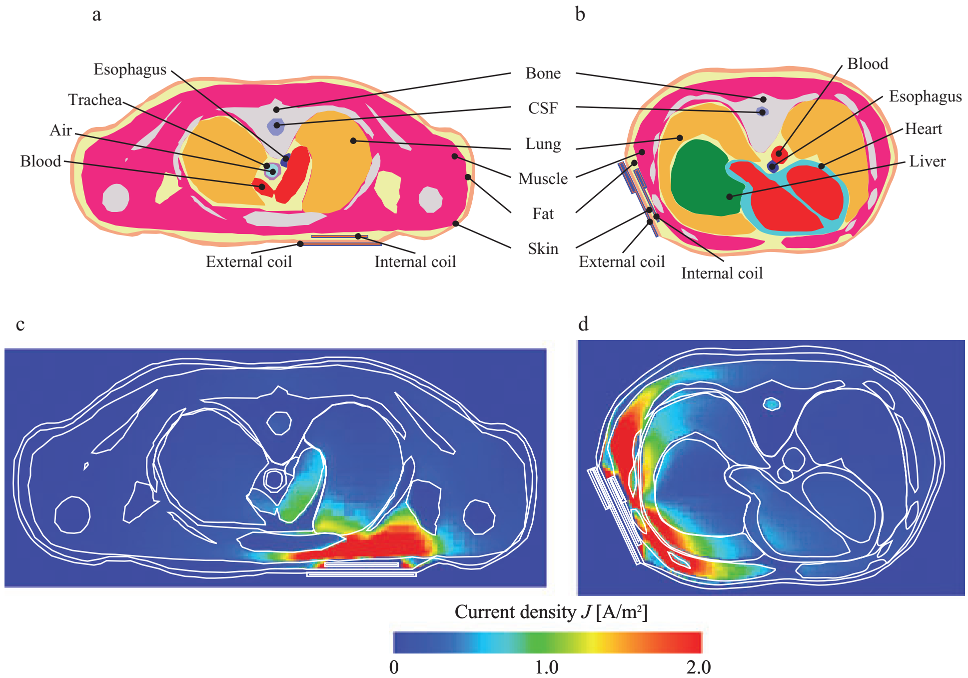


**FIG. 10.** (a) Cross-section of model 1. (b) Cross-section of model 2. (c) Current density distribution for model 1. (d) Current density distribution for model 2. CSF, cerebrospinal fluid.

relative permittivity is high ($\sigma = 0.461$, $\varepsilon_r = 3110$) is modeled as a rectangular parallelepiped with dimensions 300 × 300 × 100 mm (shown in pink). The bone with low conductivity or relative permittivity ($\sigma = 0.023$, $\varepsilon_r = 168$) is modeled as a cylinder with axis: 15 mm and height: 300 mm (shown in gray). The air-core coil (diameter 90 mm) is placed at a distance of 5 mm from the muscle. Figure 9c,d shows the simulated result obtained with the simple models 1 and 2. The electric field in simple model 2 is higher than that in simple model 1. In the simple model 2, the range in the electric field in the vicinity of $E = 2$ V/m is wide (shown in green). This result shows that the electric field $E$ increases around an organ with low conductivity or relative permittivity. Figure 10 shows the comparison of $J$ values of model 1 and model 2 on the basis of the results of the abovementioned analysis. In model 2 (Fig. 10b), the bone distribution near the air-core coils is greater as compared with that in model 1 (Fig. 10a). Therefore, $E$ increases around the bone in model 2. It is opined that the air-core coil used for the TETS should not be implanted near complex tissues (e.g., the serratus anterior muscle on the rib, etc.) because reflection of the electric field is repeated around the tissues.

The results obtained using model 2 exceed the limiting value prescribed by the ICNIRP; however, this guideline value has sufficient margin of safety from the threshold value. Therefore, it is possible to use either model safely if it is used very carefully.

## CONCLUSIONS

We used a human body model including 24 organs and calculated SAR and $J$ values in each of these organs during energy transmission to an artificial heart. Then, we analyzed the changes in the electromagnetic influence of the TETS on organs by changing the air-core coil arrangement.

We found that SAR remains within the limit for general public exposure as prescribed by the ICNIRP, and that $J$ remains within the limit for occupational exposure as prescribed by the ICNIRP. In addition, we found that electromagnetic influence of the TETS on biological tissues changed with the air-core coil arrangement. It is opined that the TETS should not be implanted near intricate tissues such as the serratus anterior muscle on the rib, etc., because reflection of the electric field is repeated around those tissues.

Hence, when selecting the location of an air-core coil for TETS, it is necessary to consider the influence of the electromagnetic field on biological tissue; this technique using MRI-based human body model is effective in the analysis of SAR and current density. In our future research, we plan to investigate the SAR and *J* values considering them as the components of the artificial heart system (blood pump, control device, energy source, and battery).

**Acknowledgements:** The authors would like to thank CST AG and AET, Inc. for their useful suggestions and assistance with regard to the electromagnetic simulator (MicroStripes).

## REFERENCES

1. Nishinaka T, Schima H, Roethy W, et al. The DuraHeart VAD, a magnetically levitated centrifugal pump. *Circ J* 2006;70: 1421–5.
2. Frazier OH, Myers TJ, Jarvik RK, et al. Research and development of an implantable, axial-flow left ventricular assist device: the Jarvik 2000 heart. *Ann Thorac Surg* 2001;71:S125–32.
3. Mario CD, Leah BE, Marshall IH, et al. Circulatory support device database of the International Society for Heart and Lung Transplantation: third annual report—2005. *J Heart Lung Transplant* 2005;24:1182–7.
4. Schuder JC, Stephenson HE, Townsend JF. Energy transfer into a closed chest by means of stationary coupling coils and a portable high-power oscillator. *Trans Am Soc Artif Intern Organs* 1961;7:327–31.
5. Fukamachi K. New technologies for mechanical circulatory support: current status and future prospects of coraide and magscrew technologies. *J Artif Organs* 2004;7:45–57.
6. Shiba K, Nukaya M, Tuji T, Koshiji K. An air-core transcutaneous energy transmission system for an artificial heart—controlling and stabilizing the output voltage using external information. *Jap Soc Med Biol Engl* 2005;43:670–6.
7. Shiba K, Nukaya M, Tsuji T, Koshiji K. Analysis of current density and specific absorption rate in biological tissue surrounding transcutaneous transformer for an artificial heart. *IEEE Trans Biomed Engl* 2008;55:205–13.
8. Abe Y, Isoyama T, Saito I, et al. Development of mechanical circulatory support devices at the University of Tokyo. *J Artif Organs* 2007;10:60–70.
9. Yamamoto T, Koshiji K, Homma A, Tatsumi E, Taenaka Y. Improvement in magnetic field immunity of externally–coupled transcutaneous energy transmission system for a totally implantable artificial heart. *J Artif Organs* 2008;11:238–40.
10. Nagaoka T, Watanabe S, Sakurai K, et al. Development of realistic high-resolution whole-body voxel models of Japanese adult male and female of average height and weight, and application of models to radio-frequency electromagnetic-field dosimetry. *Phys Med Biol* 2004;2004:1–15.
11. International Commission on Non-Ionizing Radiation Protection. Guidelines for limiting exposure to time-varying electric, magnetic, and electromagnetic fields (up to 300 GHz). *Health Phys* 1998;74:494–522.
12. Krumpholz M, Russer P. A field theoretical derivation of TLM. *IEEE Trans Microw Theory Tech* 1994;42:1660–8.
13. Institute for Applied Physics. An Internet resource for the calculation of the dielectric properties of the body tissues in the frequency range 10 Hz–100 GHz. Available at: URL: http://niremf.ifac.cnr.it/tissprop/. Accessed August 6, 2009.
14. Japan Society of Medical Electronics and Biological Engineering. *Handbook of Clinical Engineering*. Tokyo: Corona Publishers, 1984
15. Ford BJ. A new generation of cardiology: the AbioCor implantable replacement heart. *Air Med J* 2003;22:26–30.
16. El-Banayosy A, Arusoglu L, Kizner L, et al. Experience with the LionHeart left ventricular assist device in patients with end-stage heart failure. *Ann Thorac Surg* 2003;75:1469–75.
17. International Commission on Non-Ionizing Radiation Protection. Health issues related to the use of hand-held radiotelephones and base transmitters. *Health Phys* 1996; 70:587–93.